Angular distribution of Auger electrons in the decay of resonantly excited $4d^{-1}_{3/2,5/2}\,6p$ states in Xe

H. Aksela, J. Jauhiainen, E. Nõmmiste, O.-P. Sairanen, J. Karvonen, E. Kukk, and S. Aksela

Department of Physical Sciences, University of Oulu, FIN-90570 Oulu, Finland

(Received 15 April 1996)

The angular distribution of Auger electrons originating from the decay of resonantly excited $4d^{-1}6p$ states in Xe has been studied with very high photon and electron energy resolution. The resolution enhancement via the Auger resonant Raman effect has enabled to resolve the β parameters for individual resonant Auger transitions. The results are compared to previous experiments and to theoretical predictions calculated by using the multiconfigurational Dirac-Fock approach. [S1050-2947(96)01609-5]

I. INTRODUCTION

Inner-shell photoexcitation and subsequent Auger decay leads to anisotropic angular distribution of Auger electrons. Within the dipole approximation for the excitation and by assuming a two-step description of the Auger process, the angular distribution parameter β equals $\alpha_2 \mathcal{A}_{20}$, where $\mathcal{A}_{20}$ is the alignment of the excited state and α_2 is the intrinsic anisotropy of the Auger decay [1]. In photoexcitation from ground-state $J_0 = 0^+$ to $J_i = 1^-$ state using linearly polarized photons, substates with only one projection $M_i = 0$ may be populated, and the alignment parameter has a photon-energy-independent value of $\mathcal{A}_{20}(J=1) = -\sqrt{2}$. This holds, e.g., in case of $nd \rightarrow (n+2)p$ resonant excitations of Kr ($n=3$) and Xe ($n=4$). As opposed to the normal Auger transitions, where the electron emission is to a large extent isotropic, β parameters ranging from -1 to 2 have been observed in case of resonant Auger transitions (for a general reference, see, e.g., [2]).

Several theoretical studies have been published concerning the angular anisotropy of the resonant Auger decay in Kr and Xe [3–7]. Although the anisotropy is rather well understood in general, some Auger lines are known to exhibit strong deviation from predicted values. In this work, we will compare the experimental results with the most sophisticated theoretical predictions reported so far [7]. These results were generated by using the multiconfigurational Dirac-Fock (MCDF) wave functions [8]. The calculations took into account the configuration interaction both in the initial and final ionic states of the decay (ISCI and FISCI). The exchange interaction between the continuum and core electrons was also taken into account in these computations whereas in the earlier works [3–6] it, together with ISCI, was neglected. The different approximations will not be discussed in detail here but the reader is referred to Ref. [7].

For further development of the theory, a comparison with accurate experimental β values is very important. Only few studies have been reported so far (see Refs. [9–11]). These works have suffered, to some extent, from relatively poor resolution and statistics. Also the values from those experiments differ considerably. The present results hopefully clarify some of the existing discrepancies. Our main advantage here is the very high photon and electron energy reso-

lution which has enabled us to resolve most of the transitions between individual initial and final states. In order to achieve this level of resolution, the Auger resonant Raman effect was utilized [12], i.e., the $4d^{-1}6p$ resonances were excited with a photon band that was considerably narrower than the natural width of the resonant state. Thus the experimental line width is no more determined by the lifetime broadening of the excited state. On the other hand, due to inaccurate electron intensity calibration, our β parameters rely heavily on existing results and cannot be regarded as completely independent.

Very recently the β parameters for Kr $3d^{-1}5p \rightarrow 4p^4 5p$ resonant Auger transitions were determined [13] using the same experimental apparatus [14] as in this work. The agreement between the calculated and experimental β parameters was found to be good in most cases. Some individual β's were observed to be sensitive to ISCI and FISCI. In a parallel study, the relative intensities of the resonant Auger lines were also found to be affected by electron correlation [15]. Therefore, in addition to the β's, also the partial decay rates and energy splittings have to be taken into account when comparing experimental results with theory. It is possible to arrive at a better theoretical description of the electron correlation effects by combining information from these different sources.

We would like to continue this project by presenting in this study the β parameters for the Xe $4d^{-1}6p \rightarrow 5p^4 6p$ transitions. The main purpose here is to present high-resolution experimental data and to compare them with the results predicted by the MCDF calculations. These results are also complementary to the recently published angular-independent studies of Xe resonant Auger transitions [16–18].

II. EXPERIMENT

The experiments were performed at the Finnish beamline (BL51) at the MAX-Laboratory in Lund, Sweden. A detailed description of the beamline has been published elsewhere [19]. Briefly, it uses synchrotron radiation from an undulator [20] operating in the 60–600 eV photon-energy range and it has a modified SX-700 plane grating monochromator [21] with a plane elliptical focusing mirror. Recently, a new end station [14] equipped with an SES-200 hemispherical elec-
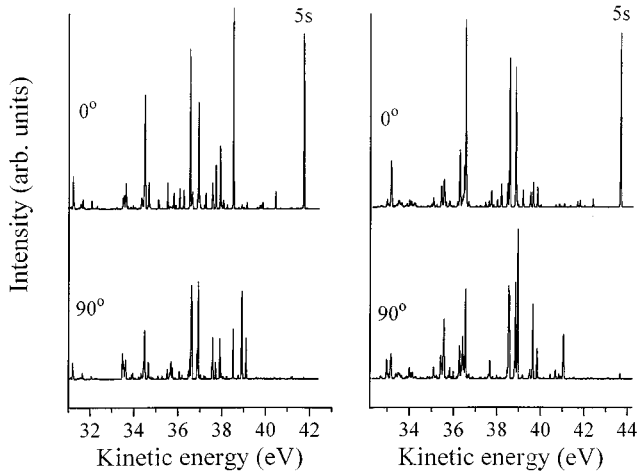
FIG. 1. Left: The $4d_{5/2}^{-1}6p \rightarrow 5p^4 6p$ resonant Auger spectrum of Xe excited by 65.110 eV photons. Right: The $4d_{3/2}^{-1}6p \rightarrow 5p^4 6p$ resonant Auger spectrum excited by 67.039 eV photons. The angle between the lens axis and the electric-field vector of incoming radiation is also shown in each spectrum.

tron spectrometer [22] has been installed at the beamline. In order to allow angle-resolved measurements, the spectrometer can be rotated in a plane perpendicular to the direction of the photon beam. An ultimate energy resolution of better than 14 meV full width at half maximum (FWHM) has been achieved, although the total line width in the present measurements was in the range of 28–33 meV which allowed us to resolve the different fine-structure components with reasonable intensity.

In these measurements a specially designed gas cell was used. The position of the gas cell was fixed relative to the lens. This ensured that the emitted electrons always entered the lens at correct angles. The position of the photon spot inside the gas cell, on the other hand, could not be fully controlled due to changes in the position of the electron beam inside the storage ring. The photon flux was monitored by a photodiode which was mounted on the rear end of the gas cell.

In most experimental angle-resolved studies so far, the β parameters have been determined by simultaneous measurement of two or more angles (see, e.g., Ref. [23]). This approach is preferable because no additional calibration measurements are needed. The present experimental setup did not allow this kind of arrangement since only one angle at a time could be recorded. Therefore, the electron spectra measured at different angles were normalized by assuming the β parameters for some lines to be known. This procedure will be described in the following section.

III. RESULTS AND DISCUSSION

A. Experimental results

1. General

The angular distribution parameters for the $4d^{-1}6p \rightarrow 5p^4 6p$ spectator resonant Auger transitions were determined by measuring the electron spectra at 0°, 54.7°, and 90° with respect to the polarization plane. The overview spectra
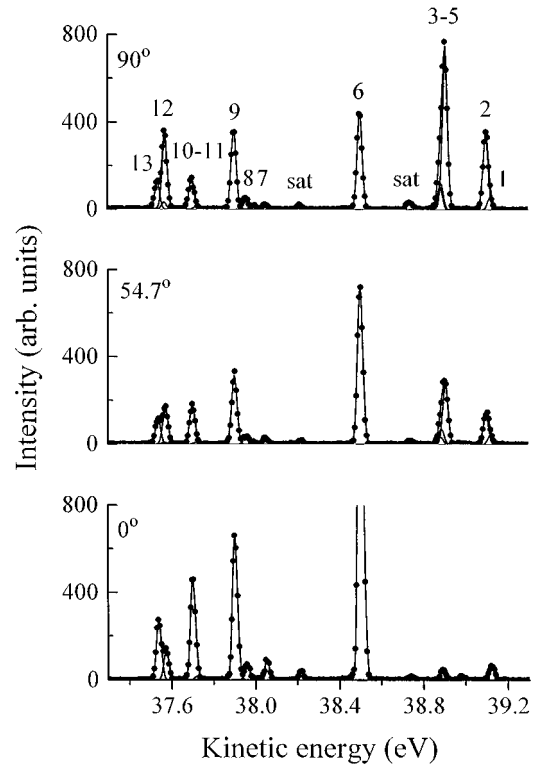
FIG. 2. Kinetic-energy region of the $4d_{5/2}^{-1}6p \rightarrow 5p^4({}^3P)6p$ resonant Auger transitions measured at 0°, 54.7°, and 90°.

are shown in Fig. 1. Details of the curve fitting are displayed in Figs. 2–5. The degree of linear polarization was estimated to be above 99%. This can be seen as an almost complete absence of the Xe 5s photoelectron line in the spectrum mea-
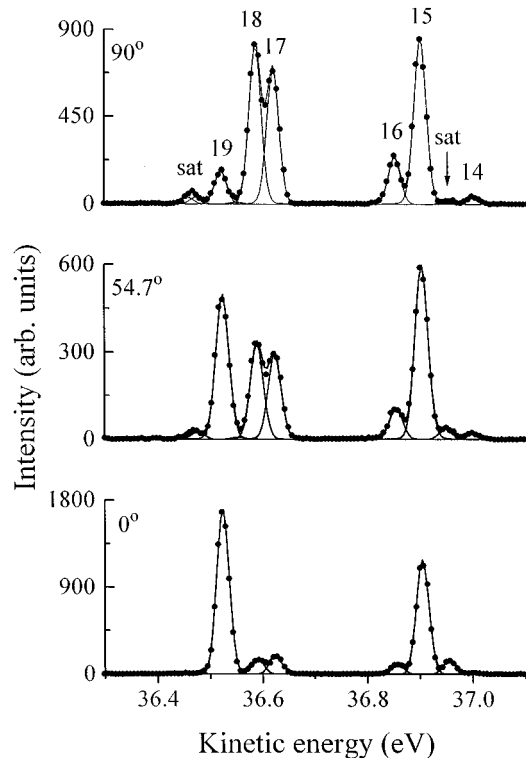
FIG. 3. Kinetic-energy region of the $4d_{5/2}^{-1}6p \rightarrow 5p^4({}^1D)6p$ resonant Auger transitions measured at 0°, 54.7°, and 90°.

TABLE I. Experimental angular distribution parameter β for Xe $4d^{-1}6p \to 5p^{-2}6p$ resonant Auger transitions. An asterisk indicates that the β's for these transitions could not be determined; see text for details. Lines with no error estimation were used for calibration.

Line no:	Final state	Binding energy (eV)	β $4d_{5/2}^{-1}6p$	β $4d_{3/2}^{-1}6p$
1	$5p^{-2}(^3P)6p\ ^4P_{3/2}$	25.991	0.32(10)	−0.44(15)
2	$5p^{-2}(^3P)6p\ ^4P_{5/2}$	26.012	−0.97(2)	−0.94(6)
3	$5p^{-2}(^3P)6p\ ^2D_{5/2}$	26.204	−0.97(2)	*
4	$5p^{-2}(^3P)6p\ ^2S_{1/2}$	26.224		
			}-0.61(12)	}0.6(2)
5	$5p^{-2}(^3P)6p\ ^4D_{7/2}$	26.228		
6	$5p^{-2}(^3P)6p\ ^2P_{3/2}$	26.609	1.27(2)	−0.6(3)
7	$5p^{-2}(^3P)6p\ ^2P_{1/2}$	27.060	1.09(10)	1.2(3)
8	$5p^{-2}(^3P)6p\ ^4P_{1/2}$	27.155	0.43(2)	*
9	$5p^{-2}(^3P)6p\ ^2D_{3/2}$	27.211	0.61(2)	0.38(6)
10	$5p^{-2}(^3P)6p\ ^4D_{5/2}$	27.394	0.51(10)	−0.7(3)
11	$5p^{-2}(^3P)6p\ ^4S_{3/2}$	27.412	1.03(2)	−0.09(8)
12	$5p^{-2}(^3P)6p\ ^4D_{3/2}$	27.540	−0.39(2)	1.04(5)
13	$5p^{-2}(^3P)6p\ ^4D_{1/2}$	27.575	0.76(3)	0.1(2)
14	$5p^{-2}(^1D)6p\ ^2F_{5/2}$	28.109	−0.3(2)	−0.9(1)
15	$5p^{-2}(^1D)6p\ ^2P_{3/2}$	28.208	0.39(4)	0.84(9)
16	$5p^{-2}(^1D)6p\ ^2F_{7/2}$	28.257	−0.4(2)	*
17	$5p^{-2}(^1D)6p\ ^2D_{3/2}$	28.489	−0.62(10)	0.97(10)
18	$5p^{-2}(^1D)6p\ ^2D_{5/2}$	28.523	−0.75(12)	−0.35(4)
19	$5p^{-2}(^1D)6p\ ^2P_{1/2}$	28.589	1.55(8)	1.12(10)
20	$5p^{-2}(^1S)6p\ ^2P_{1/2}$	30.508	*	1.00
21	$5p^{-2}(^1S)6p\ ^2P_{3/2}$	30.631	0.93	−0.18(13)
22	$5p^{-2}(^1S)6p\ ^2P_{3/2}$	30.654	0.5	−0.8(2)

sured at 90°. The assignments as well as energy positions for the resonant Auger lines were taken from Ref. [17]. The spectra were least-squares fitted using Voigt functions. The line shapes were constrained to be the same for all lines within each spectrum. Total line widths (FWHM) of about 31 ± 3 meV were obtained which roughly corresponds to 29 meV and 8 meV spectrometer and monochromator contributions, respectively. The results are summarized in Table I. In order to compare the present experimental results with the previous studies, we have also calculated intensity-weighted sums of β parameters in Table II. The peak labeling is similar to that used in the previous works in order to make the

comparison more straightforward. The average β's as well as the error limits in Table I were obtained after careful study of spectra measured under different conditions.

One additional problem in these measurements was the decreasing spectrometer transmission as a function of kinetic energy of the emitted electrons. If only the intensities at the magic angle (54.7°) are needed, the transmission function can be obtained in a simple way, as described in Ref. [24]. In case of angle-resolved measurements the problems become much more severe because two or more analyzer angles are needed to determine the β's. In practice each angle has its own transmission function, which in the present case can be

TABLE II. Intensity-weighted sums of β parameters for Xe $4d^{-1}6p \to 5p^46p$ Auger transitions. Line numbers refer to Table I. The peak labeling in the first column is the same as in Refs. [10] and [9].

Peak	Lines included	$4d_{5/2}^{-1}6p$ Ref. [10]	$4d_{5/2}^{-1}6p$ Ref. [9]	$4d_{5/2}^{-1}6p$ This work	$4d_{3/2}^{-1}6p$ Ref. [25]	$4d_{3/2}^{-1}6p$ Ref. [9]	$4d_{3/2}^{-1}6p$ This work
1a	1,2	−0.60(3)	−0.88	−0.66	−0.8		−0.74
1b	3–5	−0.90(2)	−0.93	−0.75	0.2	−0.67(1a+1b)	0.19
1c	6	1.31(2)	0.82	1.27	−0.4	−0.38	−0.55
2a	7–9	0.58(2)	0.26	0.64			
2b	10–13	0.54(3)	0.16	0.46	0.35(2a+2b)	0.14(2a+2b)	0.17(2a+2b)
3a	14–16	0.23(2)	−0.02	0.25			
3b	17–19	0.33(5)	−0.09	0.31	0.5(3a+3b)	0.32(3a+3b)	0.36(3a+3b)
5	20–22	0.83(5)	0.51	0.81	1.0	0.89	0.74

TABLE III. Calculated angular-anisotropy parameters $\beta = \alpha_2 \mathcal{A}_{20}$ for Xe $4d_{5/2}^{-1} 6p \rightarrow 5p^{-2} 6p$ Auger transitions. The line numbers refer to Table I. F indicates single-channel results obtained using final-state orbitals and excluding the exchange for the continuum electron. ISCI was computed using final-state orbitals. FE is the same as F but the exchange was included. In FEI, ISCI was calculated using initial-state orbitals. IE indicates single-channel values obtained using initial-state orbitals with exchange. FISCI was calculated using initial state orbitals.

Line no:	F	FE	IE	FEI	Chen
1	1.005	1.029	1.016	1.045	0.984
2	−1.000	−0.995	−0.996	−0.995	−1.000
3	−1.000	−0.996	−0.996	−0.996	−1.000
4	−0.089	−0.447	−0.092	−0.448	0.215
5	−0.964	−0.610	−0.665	−0.589	−0.973
6	0.971	1.025	1.093	1.031	1.018
7	0.965	0.984	1.032	0.984	0.962
8	0.634	0.237	0.715	0.233	0.771
9	0.651	0.658	0.790	0.656	0.653
10	−0.117	0.054	0.494	−0.188	−0.331
11	0.810	0.736	0.835	0.745	0.955
12	−0.584	−0.556	−0.996	−0.535	−0.860
13	0.837	0.595	0.906	0.592	0.935
14	−0.819	−0.851	−0.869	−0.876	−0.860
15	0.046	0.151	−0.078	0.176	0.073
16	0.090	0.256	0.218	0.246	0.052
17	−0.654	−0.517	−0.310	−0.553	−0.529
18	−0.860	−0.872	−0.877	−0.887	−0.882
19	1.366	1.506	1.517	1.503	1.307
20	0.504	−0.233	0.927	0.130	−0.139
21,22	0.817	0.801	0.810	0.828	0.847

approximated by a straight line with a negative slope. In a recent study [13], the transmission functions were determined with the help of the well-known Ne 2p photoionization cross sections and β parameters. Because the minimum photon energy that can be reached at BL51 is about 60 eV, we could not use this method in the case of Xe due to very low kinetic energies of Auger electrons. Therefore, the transmission correction was obtained simultaneously with the actual β determination by assuming the β parameters for the transitions to the $5p^{-2}(^{1}S)6p$ final-state parent multiplets to be 0.81 (intensity-weighted sum of β's of lines 21 and 22) and 1.00 (line 20) in the decay after the $4d_{5/2} \rightarrow 6p$ and $4d_{3/2} \rightarrow 6p$ excitations, respectively. These assumptions are supported both by the experimental studies of Kämmerling, Krässig, and Schmidt (see Table II) as well as by the theoretical predictions of Tulkki *et al.* (see Tables III and IV). Another line for which the β parameter was assumed to be known was the 5s photoelectron line ($\beta \approx 2$ well above the 5s threshold). If the excited state decays via a participator transition the 5s photoelectron line can not be used for normalization. According to the calculated results of Ref. [7], the participator decay probability is much smaller than the spectator decay.

2. The $4d_{5/2}^{-1}6p \rightarrow 5p^4 6p$ transitions

The curve fitting results for the $4d_{5/2}^{-1}6p \rightarrow 5p^4(^{3}P)6p$ transitions are displayed in Fig. 2. As already pointed out by

Carlson *et al.* [9], many of these lines apparently have highly negative β values. Lines 1 and 2 are very close to each other and the determination of their β's is only possible if their accurate energy positions are known. Because the angle-integrated intensity of line 1 is very low, its angular behavior cannot be determined very accurately. Line 2, on the other hand, clearly possesses a highly negative β value. Lines 3, 4, and 5 are located very close to each other, too. Also in this case one of them clearly has β close to −1, which according to the energy positions given in Ref. [16,17] is line 3. Although lines 4 and 5 were fitted separately we could not extract separate β parameters for them. Line 6 is the most intense one in the ^{3}P parent. Our β value of 1.27(2) is in good agreement with Kämmerling, Krässig, and Schmidt [β=1.31(2)]. Because this line is relatively well resolved we can conclude that our method to determine the β's, although it involves some inaccuracies, is correct. Lines 7 and 10 have very low intensity which is reflected as an increase in their error limits. For lines 8, 9, 11, and 12 the β parameters are more accurate because they are relatively well resolved and intense.

Our results in the case of the ^{1}D parent (Fig. 3) are again in good agreement with Kämmerling's values [10]. In the case of peak 3a, the β value mainly originates from line 15 since both line 16 and especially line 14 are weak. One 5s satellite line is located between lines 14 and 15, which is responsible for the very high error limits for line 14 in Table I. Peak 3b consists of three resonant Auger lines, too. Evidently lines 17 and 18 must have negative and mutually very similar β coefficients whereas for line 19 the β is highly positive.

In principle, one would expect only two components in the case of $5p^4(^{1}S)6p$ final states, namely, $(^{1}S)6p\ ^{2}P_{1/2}$ and $(^{1}S)6p\ ^{2}P_{3/2}$. Only the latter of these is known to gain intensity. Aksela *et al.* [17] observed two closely spaced lines (21 and 22) and assigned both of them to the $(^{1}S)6p\ ^{2}P_{3/2}$ state. The redistribution of intensity was attributed to the final ionic state configuration interaction (FISCI) between the $(5s5p)^{-2}6p$ and $(5s5p)^{-2}4f$ final-state configurations. We have used this interpretation here as well. Therefore the β value that was needed to obtain the transmission correction (0.81) was determined from the intensity-weighted sum of β's for lines 21 and 22.

3. The $4d_{3/2}^{-1}6p \rightarrow 5p^4 6p$ transitions

Here the comparison with previous studies is more complicated due to the lack of reliable reference data and the scattering between different experiments. In their paper Hergenhahn, Kabachnik, and Lohmann [3] quote still unpublished experimental β's from Becker [25]. Much of the same general discussion as in the case of $4d_{5/2} \rightarrow 6p$ excitation is valid here, too. The intensity of the ^{3}P parent multiplet (Fig. 4) is very low at every angle and we could not determine β's for lines 3 and 8. For many lines the uncertainties are very pronounced, as seen in Table I. The results for the ^{1}D parent (Fig. 5) should be more reliable. There seems to be a previously unresolved satellite line between lines 15 and 16 which makes the determination of β parameter for line 16 very inaccurate.

It must be pointed out that due to moderate resolution in Refs. [9] and [11], their β's for the $5p^{-2}(^{1}S)6p$ final state

TABLE IV. Calculated $\beta = \alpha_2 \mathcal{A}_{20}$ for Xe $4d_{3/2}^{-1}6p \rightarrow 5p^{-2}6p$ transitions. The line numbers refer to Table I. The computational approximations are the same as in Table III. In approximation FEO, ISCI was neglected.

		Excited state						
		"Lower"				"Upper"		
Line no:	FE	FEI	FEO	Chen	FE	FEI	FEO	Chen
1	−0.087	−0.080	−0.084	0.448	−0.094	−0.138	−0.035	0.393
2	−0.978	−0.831	−0.506	−0.996	0.314	0.230	−0.761	−0.232
3	0.725	0.377	−0.349	0.019	−0.954	−0.931	−0.363	−0.952
4	−0.200	−0.009	0.992	−0.035	−0.437	−0.432	−0.362	−0.426
5	−0.166	−0.197	0.000	0.146	−0.192	−0.203	−0.216	0.140
6	−0.693	0.324	1.237	−0.946	1.294	1.188	0.869	1.020
7	1.121	1.006	0.991	0.986	0.980	0.973	0.956	1.007
8	0.581	0.705	1.249	0.854	0.126	0.324	0.432	0.669
9	0.795	0.710	0.622	0.761	0.424	−0.018	0.626	0.054
10	−0.965	−0.962	0.038	−0.955	−0.968	−0.966	−0.965	−0.957
11	−0.501	−0.291	−0.086	0.298	0.276	0.783	−0.554	0.914
12	0.562	0.488	0.200	1.030	0.982	0.776	0.686	0.725
13	0.792	0.846	0.988	0.935	0.244	0.603	0.702	0.898
14	0.403	−0.054	−0.352	−0.436	−0.694	−0.918	0.451	−0.994
15	−0.338	0.443	1.031	0.274	0.886	0.251	−0.643	0.718
16	−0.845	−0.831	0.000	−0.660	−0.835	−0.830	−0.823	−0.659
17	0.981	0.950	0.777	0.827	0.294	−0.402	−0.307	−0.907
18	−0.163	−0.722	−0.317	−0.686	1.386	0.987	0.542	0.793
19	0.568	0.503	1.155	0.851	0.608	0.579	0.552	0.810
20	1.006	1.001	0.998	1.003	0.993	0.987	0.683	0.990
21,22	−0.794	−0.888	0.685	−0.871	−0.651	−0.712	−0.759	−0.707

also include some contribution from the $5p^{-2}(^1D)7p$ shake-up final states which are located in the same kinetic-energy region. In this work, we were able to resolve the structure in detail and the shake-up contribution is not included in our sum of β's (0.74) in Table II. This may explain why our value is considerably lower than that given in Refs. [9] and [11]. The corresponding shake-up states are not so strongly populated in the decay of the $4d_{5/2}^{-1}6p$ resonance [18] and therefore our sum of β's for the $5p^{-2}(^1S)6p$ final state is in better agreement with the other works.

B. Results of MCDF calculations and comparison with experiment

1. The $4d_{5/2}^{-1}6p \rightarrow 5p^46p$ transitions

Angular anisotropy is a powerful tool to study the influence of various many-electron effects to Auger decay dynamics. For instance, the impact of exchange interaction between bound and continuum electrons to the β parameters shows up as a difference between the F (exchange omitted) and FE (exchange included) values. FISCI is the main reason if the IE and FE values differ since in IE approach the mixing of final ionic states is obtained with initial-state orbitals but in FE with final-state orbitals. The influence of ISCI is seen by comparing the FEO values (ISCI omitted) with the FE (ISCI predicted with final-state basis set) and with the FEI (initial-state basis set) values.

As the theoretical β values in Tables III and IV are compared with each other, different trends show up. There are

several transitions for which the β parameters remain about the same in spite of the fact that FISCI, ISCI or exchange interaction was taken into account in a different way. If the transitions are dominated by only one transition amplitude, the electron correlation effects do not influence the angular anisotropy. Such model-independent β values are useful in calibrating the experimental values. In the decay of the $4d_{5/2}^{-1}6p$ excited state, the transitions to the states $5p^{-2}(^3P)6p$ $^4P_{5/2}$ (line 2), $5p^{-2}(^3P)6p$ $^2D_{5/2}$ (line 3), $5p^{-2}(^1D)6p$ $^2F_{5/2}$ (line 14), and $5p^{-2}(^1D)6p$ $^2D_{5/2}$ (line 18) are principally determined by the $\epsilon d_{5/2}$ partial wave. This explains their insensitivity to the methods to generate the wave functions (see Table III). Unfortunately, line 14 is weak which hampers its use for calibration purposes. Weakly model-dependent β values for lines 1, 6, 7, 9, 11, 19, and 21 are also useful when experiment is compared with theory. Pronounced disagreements in such cases would be surprising.

The interference between the $\epsilon d_{3/2}$ and $\epsilon g_{7/2}$ amplitudes gives rise to a large scattering in the β parameters for lines 5 and 10. In the case of line 4, the $\epsilon s_{1/2}$ and $\epsilon d_{3/2}$ amplitudes are also of the same order of magnitude. Since lines 4 and 5 are close to each other it is difficult to obtain their individual β values. The β parameter for the $5p^{-2}(^1D)6p$ $^2F_{7/2}$ state (line 16) is determined by the $\epsilon g_{9/2}$ partial wave. This amplitude is very sensitive to the exchange interaction between the continuum and core electrons. The β parameter does not show such a strong dependence on the exchange interaction as the partial decay rate [16]. Relative intensities of lines are

usually better suited to testing the capability of the theory to take the exchange interaction into account.

As the theory is compared with the experiment, some conclusions can be drawn. When the calculated β is model independent, the experimental value is usually very close to the calculated one. For lines where there is considerable scattering in the β values between calculations, none of the models is capable of predicting the experiment correctly. However, calculations where the exchange interaction is included (FE, IE, FEI) seem to reproduce the experiment somewhat better than the models, where it is omitted. For instance, the FE approach seems to move the β for the peak composed of lines 4 and 5 to the direction of the experimental value as compared to the approximation F. The same holds for line 10, even though the FE calculations still underestimate the β. The basis set seems to play an important role here: IE approach gives the best agreement with experiment for line 10. This line is, however, very weak which makes it difficult to determine its β correctly by both experiment and theory. If the relaxation reduces the contributing partial waves by a constant factor the effect to the angular dependence is small. If one of the waves, however, is sensitive to the orbital-collapse phenomenon the angular anisotropy may be affected. In future theoretical work the influence of relaxation to the angular distribution needs to be studied thoroughly.

All the calculations seem to predict a wrong sign for the β parameter of line 16. Partial decay rate of this transition was also heavily overestimated by theory [16]. This indicates that the $\epsilon g_{9/2}$ partial wave does not play such a dominant role in the transition to the $5p^{-2}(^1D)6p\ ^2F_{7/2}$ state as estimated by theory. If the mixing of continuum channels is of importance here, it needs to be studied separately.
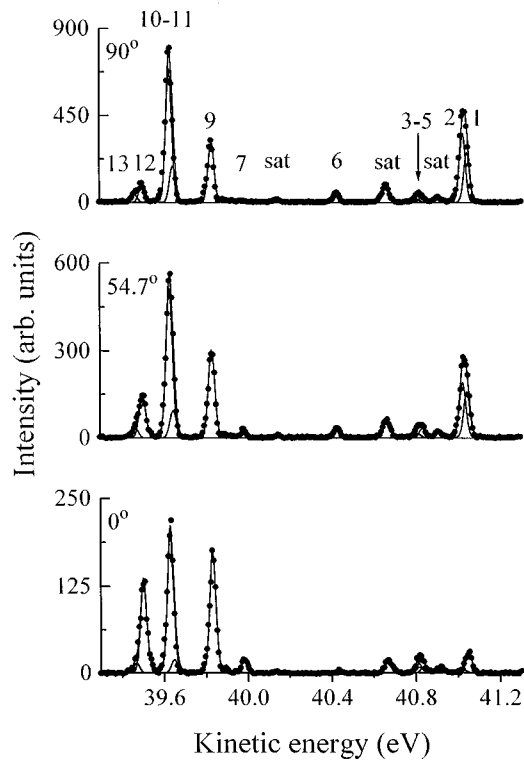
All the calculations give large negative β values for line 17, being in fairly good agreement with the experiment. FISCI is important here but what is interesting is that the partial decay rates [16] scatter much more than the β values. Thus the relative line intensities are often more sensitive to FISCI than the β parameters. There are surprising discrepancies between experiment and theory in the case of lines 1 and 14. These lines are, however, weak and line 1 lies close to line 2. For weak transitions the experiment is less accurate but the β's are also easily affected by possible inaccuracies of the theoretical models.

2. The $4d_{3/2}^{-1}6p \rightarrow 4p^4 6p$ transitions

ISCI plays a very important role in the decay of the $4d_{3/2}^{-1}6p$ excited state. In Refs. [5,6] the ISCI was entirely neglected. Due to strong mixing of the $4d_{3/2}^{-1}6p_{1/2}$, $J=1$ and $4d_{3/2}^{-1}6p_{3/2}$, $J=1$ states, the single-configuration description fails to describe the excited states. The states are therefore referred to as ''lower'' and ''upper,'' respectively. This labeling follows the binding-energy ordering of the states as obtained by the MCDF calculations.

For angular anisotropy, the predictions F, FEI, and FEO differ considerably from each other (see Table IV). Only for lines 7 and 20 the β parameters are practically independent on ISCI. A few lines in ''lower'' and ''upper'' excited states are only weakly sensitive to the details of calculations. The ''lower'' excited state was predicted [7] to be dominantly populated in photoexcitation. In the decay of the ''lower'' state the β's of the transitions 2, 9, 13, and 17 seem not to vary very much in different approximations. These transitions are governed by one transition amplitude only. FISCI plays some role, however, and the transitions are also some-

FIG. 4. Kinetic-energy region of the $4d_{3/2}^{-1}6p \rightarrow 5p^4(^3P)6p$ resonant Auger transitions measured at $0°$, $54.7°$, and $90°$.
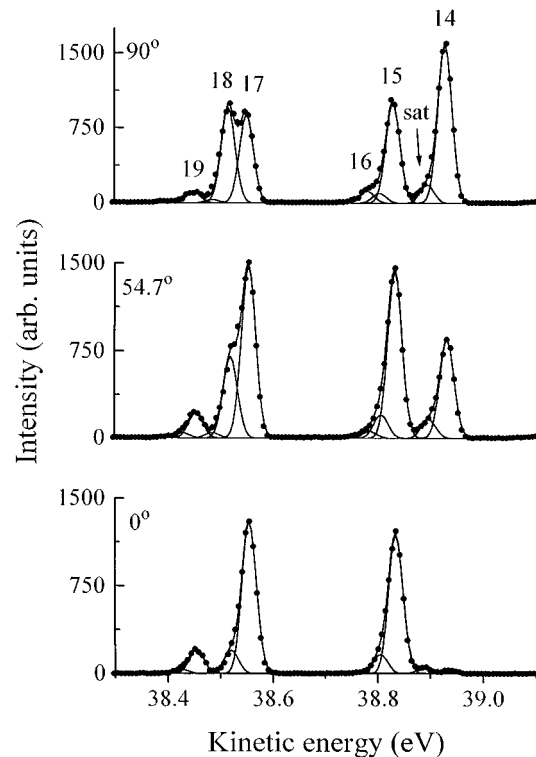
FIG. 5. Kinetic-energy region of the $4d_{3/2}^{-1}6p \rightarrow 5p^4(^1D)6p$ resonant Auger transitions measured at $0°$, $54.7°$, and $90°$.

what affected by ISCI as seen when the FE, FEI, and FEO values (Table IV) are compared to each other. Only in the case of lines 2 and 17 the calculated (especially the FE and FEI predictions) and experimental β values agree fairly well.

Two partial waves are of the same order of magnitude in the case of lines 5, 6, 15, and 16. The theoretical β parameters differ so much from the experimental ones that further theoretical work is clearly needed in order to find a proper ratio of partial amplitudes and their phases. ISCI is also important for all these transitions, making them very sensitive test cases for future calculations.

The FEI may be considered as the best one of the approximations since both ISCI and FISCI are taken into account in a most sophisticated way so far. If the FEI values for the ''lower'' and ''upper'' state are compared to the experimental β's, for most of the lines the values of the ''lower'' state are closer to the experiment. This supports the assumption that the resonant Auger process takes place via the ''lower'' excited state. One may accidentally find a good agreement between the experiment and a few β's of the ''upper'' state but a closer consideration shows that such β's vary heavily depending on the approximation used. Such variations indicate a large sensitivity to the electron correlation, which is not properly treated by the present calculations. According to our previous study [17], the best description so far for the partial decay rates at the $4d_{3/2}^{-1}6p$ resonance is given by the FEI approximation for the ''lower'' state. The agreement with experiment was not complete, however. In the case of β parameters the discrepancies are even larger.

C. Comparison between Kr and Xe

The $nd^{-1}(n+2)p \rightarrow (n+1)p^{-2}(n+2)p$ resonant Auger transitions in Kr ($n=3$) and Xe ($n=4$) involve similar orbitals, only the principal quantum number differs by one. Kinetic energies of Auger electrons are relatively low for both atoms: about 55–60 eV in Kr and about 35–40 eV Xe. This makes them ideal targets to study the effects of electron correlation to the decay rates and the angular anisotropy. The partial decay rates have been studied very thoroughly in both atoms [15–18,26]. Here we would like to briefly compare the β parameters, too, in order to see if more general trends can be found.

Transitions to $(n+1)^{-2}(^3P)(n+2)p$ $^4P_{5/2}$ and $(n+1)^{-2}(^3P)(n+2)p$ $^2D_{5/2}$ final states in both atoms yield β values very close to -1. This is consistent with the model that the angular anisotropy is governed only by the coupling of the angular momenta. As pointed out in Ref. [13], the dominance of the $\epsilon d_{5/2}$ partial wave causes the angular dis-

tribution of these transitions to be insensitive to FISCI as well as to FCSCI (final continuum state CI). Two other transitions are also dominated by the $\epsilon d_{5/2}$ partial wave, namely, lines 14 and 18. Unfortunately, the former is very weak in Kr, while the latter cannot be properly resolved in Xe.

Transitions with $J=3/2$ were found to be well reproduced by calculations in [13] and the same general trend can be seen here, too. An interesting observation is that in Xe, calculations fail to estimate the β for line 16, which is dominated by the $\epsilon g_{9/2}$ partial wave. In Kr, however, the calculations are in fairly good agreement with the experiment. The $\epsilon g_{9/2}$ partial wave is obviously overestimated by theory in Xe. This also demonstrates nicely the diminishing strength of exchange interaction between continuum and core electrons on going from Xe to Kr. On the other hand, hints of decreasing FCSCI on going from Kr to Xe were observed in case of normal Auger transitions [27].

Further studies on the decay of Ar $2p^{-1}4s$ resonances, where the kinetic energies of resonant Auger electrons are considerably higher (above 200 eV), are also under way. They should give more insight to the strength of electron correlation as a function of atomic mass as well as the kinetic energy of Auger electrons.

IV. CONCLUSIONS

The angular distribution parameters have been determined for the Xe $4d^{-1}6p \rightarrow 5p^{-2}6p$ resonant Auger transitions. The use of the Auger resonant Raman effect has allowed to resolve the transitions between individual initial and final states. A careful comparison between experiment and theory indicates that angular dependence is fairly well reproduced by theory at the $4d_{5/2}^{-1}6p$ resonance. ISCI has a dramatic effect on the anisotropy of Auger decay at the $4d_{3/2}^{-1}6p$ resonance but the calculations fail to reproduce it correctly. Further effort is needed to clarify all the remainig discrepancies between experiment and theory.

[1] E. G. Berezhko, and N. M. Kabachnik, J. Phys. B **10**, 2467 (1977).

[2] V. Schmidt, Rep. Prog. Phys. **55**, 1483 (1992).

[3] U. Hergenhahn, N. M. Kabachnik, and B. Lohmann, J. Phys. B **24**, 4759 (1991).

[4] U. Hergenhahn, B. Lohmann, N. M. Kabachnik, and U. Becker, J. Phys. B **26**, L117 (1993).

[5] M. H. Chen, Phys. Rev. A **47**, 3733 (1993).

[6] S. Fritzsche, Phys. Lett. A **180**, 262 (1993).

[7] J. Tulkki, H. Aksela, and N. M. Kabachnik, Phys. Rev. A **50**, 2366 (1994).

[8] I. P. Grant, B. J. McKenzie, P. H. Norrington, D. F. Mayers, and N. C. Pyper, Comput. Phys. Commun. **21**, 207 (1980).

[9] T. A. Carlson, D. R. Mullins, C. E. Beall, B. W. Yates, J. W. Taylor, D. W. Lindle, B. P. Pullen, and F. A. Grimm, Phys. Rev. Lett. **60**, 1382 (1988); T. A. Carlson, D. R. Mullins, C. E.

Beall, B. W. Yates, J. W. Taylor, D. W. Lindle, and F. A. Grimm, Phys. Rev. A **39**, 1170 (1989).

[10] B. Kämmerling, B. Krässig, and V. Schmidt, J. Phys. B **23**, 4487 (1990).

[11] C.D. Caldwell, in *X-Ray and Inner-Shell Processes, Knoxville, 1990*, Proceedings of the Fifteenth International Conference on X-Ray and Inner-Shell Processes, edited by T.A. Carlson, M.O. Krause, and S.T. Manson, AIP Conf. Proc. No. 215 (AIP, New York, 1990), p. 685.

[12] G. S. Brown, M. H. Chen, B. Crasemann, and G. E. Ice, Phys. Rev. Lett. **45**, 1937 (1980); G. B. Armen, T. Åberg, J. C. Levin, B. Crasemann, M. H. Chen, G. E. Ice, and G. S. Brown, Phys. Rev. Lett. **54** 1142 (1985); A. Kivimäki, A. Naves de Brito, S. Aksela, H. Aksela, O.-P. Sairanen, A. Ausmees, S. J. Osborne, L. B. Dantas, and S. Svensson, Phys. Rev. Lett. **71**, 4307 (1993).

[13] H. Aksela, J. Jauhiainen, E. Nõmmiste, S. Aksela, S. Sundin, A. Ausmees, and S. Svensson, Phys. Rev. A **54**, 605 (1996).

[14] S. Svensson J.-O. Forsell, H. Siegbahn, A. Ausmees, G. Bray, S. Södergren, S. Sundin, S. J. Osborne, S. Aksela, E. Nõmmiste, J. Jauhiainen, M. Jurvansuu, J. Karvonen, P. Barta, W. R. Salaneck, A. Evaldsson, M. Lögdlund, and A. Fahlman, Rev. Sci. Instrum. (to be published).

[15] H. Aksela, J. Jauhiainen, E. Kukk, E. Nõmmiste, S. Aksela, and J. Tulkki, Phys. Rev. A **53**, 290 (1995).

[16] H. Aksela, S. Aksela, O.-P. Sairanen, A. Kivimäki, A. Naves de Brito, E. Nõmmiste, J. Tulkki, S. Svensson, A. Ausmees, and S. J. Osborne, Phys. Rev. A **49**, R4269 (1994).

[17] H. Aksela, O.-P. Sairanen, S. Aksela, A. Kivimäki, A. Naves de Brito, E. Nõmmiste, J. Tulkki, A. Ausmees, S. J. Osborne, and S. Svensson, Phys. Rev. A **51**, 1291 (1995).

[18] O.-P. Sairanen, H. Aksela, S. Aksela, J. Mursu, A. Kivimäki, A. Naves de Brito, and E. Nõmmiste, J. Phys. B **28**, 4509 (1995).

[19] S. Aksela, A. Kivimäki, A. Naves de Brito, O.-P. Sairanen, S. Svensson, and J. Väyrynen, Rev. Sci. Instrum. **65**, 831 (1994); S. Aksela, A. Kivimäki, O.-P. Sairanen, A. Naves de Brito, and S. Svensson, Rev. Sci. Instrum. **66**, 1621 (1995).

[20] H. Ahola and T. Meinander, Rev. Sci. Instrum. **63**, 372 (1992); Å. Andersson, S. Werin, T. Meinander, A. Naves de Brito, and S. Aksela, Nucl. Instrum. Methods Phys. Res. A **362**, 586 (1995).

[21] R. Nyholm, S. Svensson, J. Nordgren, and A. Flodström, Nucl. Instrum. Methods A **246**, 267 (1986); S. Aksela, A. Kivimäki, R. Nyholm, and S. Svensson, Rev. Sci. Instrum. **63**, 1252 (1992).

[22] N. Mårtensson, P. Baltzer, P.A. Brühwiler, J.-O. Forsell, A. Nilsson, A. Stenborg, and B. Wannberg, J. Electron Spectrosc. Relat. Phenom. **70**, 170 (1994).

[23] H. Derenbach, C. Franke, R. Malutzki, A. Wachter, V. Schmidt, Nucl. Instrum. Methods A **260**, 258 (1987).

[24] J. Jauhiainen, A. Ausmees, A. Kivimäki, S. J. Osborne, A. Naves de Brito, S. Aksela, S. Svensson, and H. Aksela, J. Electron Spectrosc. Relat. Phenom. **69**, 181 (1994).

[25] U. Becker (unpublished), data quoted in Ref. [3].

[26] J. Jauhiainen, H. Aksela, O.-P. Sairanen, E. Nõmmiste, and S. Aksela, J. Phys. B (to be published).

[27] J. Tulkki, N. M. Kabachnik, and H. Aksela, Phys. Rev. A **48**, 1277 (1993).